Clouds and Climate: Sensitivity of Simple Systems

GRAEME L. STEPHENS AND PETER J. WEBSTER

CSIRO Division of Atmospheric Physics, Aspendale, Victoria, Australia

(Manuscript received 19 June 1980, in final form 7 October 1980)

ABSTRACT

A one-dimensional radiative convective model is used to gage the influence of clouds on simple climate systems. The radiative transfer model is developed to accommodate in a systematic and consistent manner the optical properties of a hierachy of cloud types. Cloud albedo and emissivity relationships for both ice and water clouds are introduced.

The model structure is highly sensitive to cloud height for all cloud types and particularly sensitive to water path for optically thin clouds. High thin clouds at low and middle latitudes in all seasons and all clouds at high latitudes in winter tend to warm the surface relative to the clear sky; all other clouds tend to cool the surface. The summer high-latitude effects are similar to the low- and middle-latitude situation. The model sensitivity is compounded by surface albedo effects. For a given cloud a critical surface albedo may exist at which the cloud transits from cooling the surface relative to clear-sky conditions to warming the surface when the surface albedo is increased. The critical albedos fall within the observed albedo range of real systems. The sensitivity of the model indicates that great care is necessary in developing parameterizations for the radiative structure of clouds and for surface albedos for use in climate models.

It is argued that simple energy balance models (e.g., Budyko, 1969) will be of limited use in climate research unless a cloud amount-surface temperature relationship is established. For example, the cloud-surface temperature effect will tend to buffer the Budyko surface temperature-surface albedo feedback *if* cloud amount increases with decreasing surface temperature or is independent of surface temperature but will enhance the feedback *if* the cloud-surface temperature relationship were reversed. It is concluded that the establishment of a simple cloud amount-temperature relationship will remain an elusive goal.

1. Introduction

There is little quarrel that the primary energy source of the earth's climate system is the incoming solar stream and that the major sink is the outgoing longwave stream. Controversy stems from another quarter; the manner in which the radiative stream [i.e., $F(z)$] is modulated. As the shortwave gain and the longwave loss are not usually in local balance, a three-dimensional redistribution of energy occurs as the system seeks equilibrium. Within a climate system, clouds of varying distribution, character, thickness and height appear as intrinsic features. Their roles as important modifiers of the radiation budget on either regional or planetary scales or as integral elements of feedback loops which enhance or buffer changes in a climate system is a question of concern and debate.

Of all climate constituents, clouds have the potential of exercising maximum impact on both the longwave and shortwave streams. The controversial question is whether or not clouds affect the *net* radiation stream. Cess (1976), for example, argues that the shortwave loss of energy due to cloud reflection is exactly balanced by longwave enhancement by cloud absorption. Recent studies by Ohring and Clapp (1980) suggest that the net radiation balance at the top of the atmosphere is sensitive to changes in cloud amount. Hartman and Short (1980) have shown that the quantities discussed by Cess and Ohring and Clapp are fundamentally different. For example, Cess calculated a quantity like the total derivative of net flux with cloud (i.e., dF/dQ) while Ohring and Clapp computed the sensitivity of the radiation balance to changes in cloudiness (i.e., $\partial F/\partial Q$).

However, aimed principally at the planetary-scale radiation budgets, neither the Ohring-Clapp nor Cess study addresses the problem of *regional* or *vertical* energy redistributions by cloud. This is important because energy conversions and dynamic structures critically depend on the vertical distribution of total diabatic heating to which radiational forcing is a considerable contributor (Stephens and Wilson, 1979; Webster and Stephens, 1980). Consequently, the question of the impact of clouds on the net outgoing radiation flux at the top of the atmosphere may have only a partial relevance to the impact of clouds on the climatic state of the earth system. Conceivably, the net flux at the top of the atmosphere is the radiative quantity least sensitive to changes in cloud amount. That is, a particular

0022-4928/81/020235-13$07.25

value of the net flux need not represent a unique state of the column below.

Thus, a definitive study of the cloud-climate problem has remained an elusive attainment. Observational studies have been hampered by the need to establish control situations. Similarly, because of the multi-faceted interdependencies of cloud and climate, investigations by theoretical and numerical models are equally difficult and possibly premature with current models (G. E. Hunt *et al.*, 1980). The utilization of simple energy balance models tends to be constrained by the simplicity of the adjunct radiation models and cloud parameterizations which often depend only on a single atmospheric temperature which is a prescribed and tuned function of the surface temperature (Stephens and Webster, 1979) and the neglect of all but the simplest dynamic transports.

The problems facing the larger and more sophisticated models are underlined by the study of B. G. Hunt (1978) who found the earth climate sytem, at least as simulated by a general circulation model, to be relatively insensitive to cloudiness. However, G. E. Hunt *et al.* (1980) questioned this lack of sensitivity on the basis that B. G. Hunt's model ignored certain critical feedback mechanisms in common with other general circulation models. In particular, the B. G. Hunt study neglected the relative humidity feedback in the radiation calculations.

Similar pitfalls await investigations using simpler models. For example, Stephens and Webster (1979) discussed the sensitivity of radiative forcing to both variations of cloud amount and of cloudy- and clear-sky optical properties. Within the confines of an extremely simple model they found the radiative balance to be a strong function of both cloud character and cloud height. The results allowed Stephens and Webster (1979) to make specific recommendations regarding the treatment of cloud parameterizations and radiative transfer in both simple and complex climate models. However, the major simplification of the Stephens-Webster model was a fixed-state constraint. That is, the radiation balance was calculated relative to a fixed atmospheric state for a given cloud structure such that the results could only be interpreted as an initial tendency of the atmosphere to the imposition of cloud.

In the present study the fixed-state constraint is relaxed by the introduction of a convective adjustment model which is similar to the one-dimensional model of Manabe and Wetherald (1967). However, the model differs in total form by the difference in radiative transfer schemes (see Stephens and Webster, 1979) and in the consistent manner in which both the shortwave and longwave effects of clouds are included. As distinct from Manabe and Wetherald, who held cloud albedo constant for all emissivities, a relationship is used which binds the two cloud properties via the cloud liquid-water path.

The relaxation of the fixed-state constraint increases the complexity of the Stephens-Webster model considerably. The additional complexity allows the ascertainment of whether the initial tendencies of the effect of cloud, as calculated by Stephens and Webster, are modified when the thermal structure of the system is allowed to readjust. Second, because the surface energy budget may adjust as the model procedes toward equilibrium, it introduces a second class of sensitive parameters; most notably surface albedo.

The basic aims of the study are to assess the sensitivity of a system whose complexity has been increased one step beyond the state of the Stephens-Webster system. The system represented by the present model possesses the rudiments of self adjustment (both radiative and convective) to variations in cloud type. However, the model does not allow adjustments due to the evolving dynamic state of the ocean. Horizontal transports of heat by the large-scale atmospheric motions are introduced but only in a crude climatological fashion.

In the next three sections the radiative-convective model with its attendant cloud property parameterizations will be developed. In Section 6, the sensitivity of the model structure to variations in cloud form and amount will be studied together with the related sensitivities induced by variations of surface albedo in a cloudy atmosphere.

2. The radiative transfer model

The radiative transfer model used for the determination of the shortwave fluxes is based on the scheme of Stephens and Webster (1979) which incorporates the clear air parameterizations of Lacis and Hansen (1974). The original three-layer model of Stephens and Webster is extended to 19 layers.

The longwave fluxes are calculated by an approach more consistent with present aspirations and requires the solution of the radiative transfer equations. Following Rodgers (1967),[1] we may write

$$\left.\begin{aligned} F^{\uparrow} &= \left[B_\nu(T_s)\tau_{\nu s} + \int_{\tau_{\nu s}}^{1} B_\nu(T_z)d\tau_{\nu z}\right](1-\theta) \\ &\quad + \left[F_{CT}\tau_{\nu CT} + \int_{\tau_{\nu CT}}^{1} B_\nu(T_z)d\tau_{\nu z}\right]\theta \\ F^{\downarrow} &= \left[\int_{\tau_{\nu z}}^{1} B_\nu(T_z)d\tau_{\nu z}\right] + F_{CB}\tau_{\nu CB}\theta \end{aligned}\right\}, \quad (1)$$

where T_z is the temperature of the atmosphere at any height z, $B_\nu(T_z)$ is the blackbody radiation at T_z, F_{CT} is the radiant flux (exitance) at cloud top and F_{CB} is the cloud base (exitance). Subscript s denotes

[1] The transmittance form of the radiative transfer equations is used as in Paltridge and Platt (1976) Eq. (7.5) which differs from Rodgers only in notation.

evaluation at the ground. τ_{vz} is the transmittance of the atmosphere for diffuse radiation between the reference height and the appropriate atmospheric boundary (either at the ground, cloud base, cloud top or top of the atmosphere). θ represents the fraction of sky covered by a cloud layer. Note that in the region of cloud cover, the clear-sky calculations are extended to the relevant cloud boundaries. The fluxes from the cloud boundaries (exitances) are then determined via an effective cloud emittance form given by

$$\left.\begin{aligned} F^{\uparrow}\text{ (cloud top)} &= F_0^{\uparrow}(1-\epsilon^{\uparrow}) + \epsilon^{\uparrow}\sigma T_c^4 \\ F^{\downarrow}\text{ cloud base)} &= F_0^{\downarrow}(1-\epsilon^{\downarrow}) + \epsilon^{\downarrow}\sigma T_c^4 \end{aligned}\right\}, \quad (2)$$

where $F_0^{\uparrow,\downarrow}$ are the respective incident cloud-base and cloud-top fluxes determined from (1). Thus the first term on the right-hand side of (2) represents the contribution to the exitance by the transmitted component of the incident flux and the second term is the emitted component by the cloud with a temperature T_c. The effective cloud emittances $\epsilon^{\downarrow\uparrow}$ are discussed in Section 4.

The introduction of cloud cover in (1) and in the shortwave scheme (see Stephens and Webster, 1979) implies linearity between the radiative properties in a clear and cloudy atmosphere. This is an oversimplification since nonlinear corrections are likely for albedo relationships for finite cloud types.

3. Transmittance modeling

The calculation of the transmission functions of (1) and (2) assumes critical importance in the study of climate phenomena especially when cloud processes are involved. In the following paragraphs, schemes used to calculate transmittance functions for water vapor, the water vapor–CO_2 overlap and the 9.3 μm O_3 band are discussed.

a. Water vapor transmittance

The transmittance of longwave radiation through the major water vapor absorption bands is incorporated using the greybody emissivity approach of Rodgers (1967) with the extension of Stephens and Webster (1979) to include water vapor dimer molecule (*e*-type) absorption. Pressure corrections for absorption along a pressure varying path are performed using the simple scaling approach (see Rodgers, 1967). While this approach is likely to be reasonable for water vapor absorption in the troposphere it will not be appropriate for CO_2 and O_3 absorption especially in the stratosphere.

b. Water vapor–CO_2 overlap

The water vapor–CO_2 overlap region is treated in the manner of Rodgers and Walshaw (1966) as a 200 cm^{-1} wide single interval centered at 667 cm^{-1}. Pressure corrections along the absorption path are implemented via the Curtis-Godson approximation.

c. 9.6 μm O_3 band transmission

Two major problems exist in the conventional treatment of ozone transmission which uses the two parameter Curtis-Godson approximation with the Goody random model. First, weaknesses in the Goody random model emerge when applied to spectra composed of a large number of intense lines such as exists for ozone. Second, the incorporation of pressure variations along the absorption path either by the one parameter scaling approximation used in Section 2a or the two parameter Curtis-Godson approximation are extremely inaccurate for ozone although reasonable for strong water vapor and CO_2 absorption. We follow Rodgers[2] to overcome these problems. First, the Malkmus (1967) random model is utilized which possesses a more realistic distribution for ozone. Second, a four parameter approximation is applied (after Goody, 1964). The approximation used in conjunction with the Malkmus random model provides ozone transmission results which compare well with the more complicated Kuriyan *et al.* (1977) model.

For the sensitivity studies, which form the substance of the paper, the ozone profiles for the McClatchey *et al.* (1972)[3] tropical, U.S. and subarctic winter standard atmospheres are used to represent a relatively wide range of ozone amounts and profiles (0.225 cm NTP for the tropical model to 0.15 cm NTP for the subarctic winter model).

4. Cloud-radiation parameterization

a. Low and middle clouds

The radiative properties of the low and middle cloud types were obtained using the parameterizations developed by Stephens (1978) for water clouds which provide shortwave absorption and cloud albedo for a given solar zenith angle and cloud longwave emittance. The most important feature of Stephens' parameterization is that it allows both the shortwave and longwave properties (i.e., albedo and emissivity) to be determined by one property of the cloud; the cloud water content. Mean daily zenith angles and fractional day lengths were taken from Manabe and Möller (1961).

Fig. 1a shows the relative behavior of cloud albedo and cloud emission as a function of cloud liquid-water path. The most notable feature is that the rate

[2] Rodgers, C. D., 1967: The radiative heat budget of the troposphere and the lower stratosphere. Planetary Circulation Project, Department of Meteorology, Rep. No. A2, MIT, 99 pp.

[3] McClatchey, R., R. E. Fenn, J. E. Selby, F. E. Volz and J. S. Garing, 1972: Optical properties of the atmosphere. AFCRL-72-0497, Air Force Cambridge Research Labs., Bedford, MA, 107 pp.

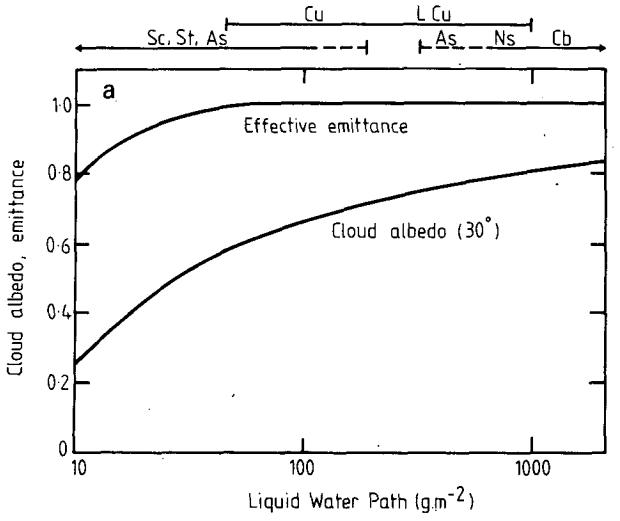

FIG. 1a. Cloud albedo and cloud effective emittance as a function of liquid-water path w for a zenith angle of 30°. Bars on upper abscissa denote approximate radiative property limits of various cloud species.

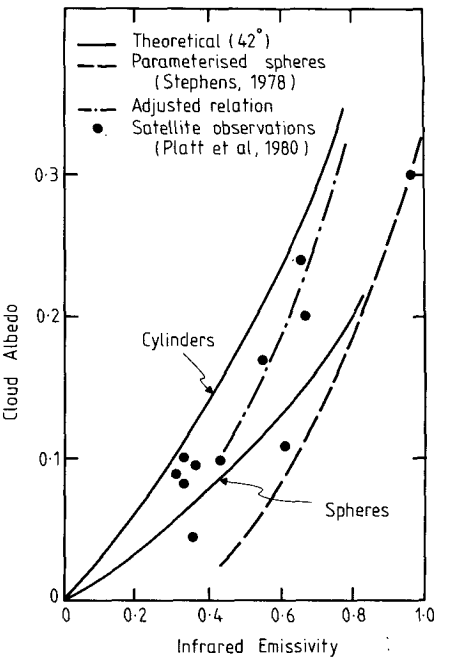

FIG. 2. Cloud albedo as a function of cloud emittance for a theoretical cloud layer composed of randomly oriented cylindrical ice crystals and spherical water droplets (solid curves). Parameterizations of Stephens (1978) are shown as dashed curves. Dots denote satellite-lidar observations of Platt *et al.* (1980).

of change of cloud albedo with increasing water path is greater than that of the effective emittance; i.e., clouds are optically black if their water paths are $\geqslant 40$ g m^{-2}, whereas a maximum value of cloud albedo is not reached until the water path exceeds 500 g m^{-2}. Consequently, an increase in the cloud-water path to values > 40 g m^{-2} will only affect the shortwave part of the radiation balance as at that water-path value the longwave emittance has already achieved its maximum value. However, if the water path were decreased to values < 40 g m^{-2}, the rate of change of cloud albedo is far greater than the decrease in emittance which will be shown to imply, in general, an increase in surface heating.

Shortwave effects are also strong functions of zenith angle. Fig. 1b illustrates the cloud albedo dependency on zenith angle for increasing liquid-water path. For thin clouds the albedo increases by over a factor of 2 between 0° and 60°. For thicker clouds the albedo increase is limited to 15–20% over the same zenith angle range.

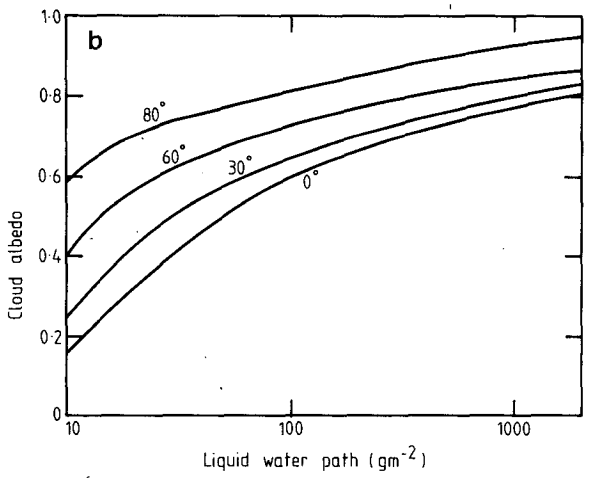

FIG. 1b. Cloud albedo as a function of liquid water path for various zenith angles.

b. High clouds

The radiative properties of high clouds are not well known, although they are improving by theoretical deduction and remote sensing of cloud properties (e.g., Stephens, 1980; Platt *et al.*, 1980). High cloud albedos (for a zenith angle of 42°) and emittances deduced from the satellite-lidar measurements of Platt *et al.* (1980) are shown on Fig. 2 (solid dots) together with theoretically calculated relationships for a model cloud layer composed of randomly oriented cylindrical crystals and spherical ice particles (Stephens, 1980). The satellite-lidar deduced values tend to fall closer to the theoretical cylinder curve. The dashed curve represents the relationship of Stephens (1978) which shows a reasonable fit with the theoretical sphere relationship (solid curve) for optically thick clouds. The relatively poor fit for optically thin clouds is due to the original parameterization being designed specifically for optically thick water drop clouds, as mentioned in the last section.

The reflectance-emittance relation assumed in the subsequent analysis is shown on Fig. 2 as the dot-dash curve. The relation was determined by assuming the cloud albedo-liquid water path parameterization of Stephens (1978) but where the ice water path is used in place of liquid-water path. The (effective) emittance–ice-water path relation is adjusted accordingly as

$$\epsilon^{\uparrow\downarrow} = 1 - \exp(-0.1w), \qquad (3)$$

where w is the ice water path (Stephens, 1980). For reasonable agreement with the relations depicted on Fig. 2, only case studies with $w > 5$ g m^{-2} are considered so that to first approximation the cloud albedo and emittance are related through the ice water path. Thus, only the ice-water path and solar zenith angle are required to describe the radiative properties of the ice cloud. Even though the validity of (3) is difficult to ascertain; observations of cirrus cloud properties are still rather rare, it does agree reasonably with the results of Cox and Griffith (1979).

A significant weakness of the parameterization of the cloud optical properties utilized in this study is the neglect of the nonlinear effects due to the finite geometric structures of partial cloud cover. However, the inclusion of such effects if far from trivial as it may be expected that the type of cloud, the structure of the cloud elements, the zenith angle and the cloud depth may be of considerable importance. In this study we assume only clear or overcast conditions and linearly extrapolate in between to compute the effects of partial cloud cover.

5. The radiative-convective model

A convective adjustment scheme similar to that of Manabe and Wetherald (1967) is coupled to the radiative transfer model and cloud parameterizations developed in the last sections to produce a one-dimensional radiative convective model (1D/RC). Radiative equilibrium is approached iteratively at all levels in the atmospheric column except where the resultant temperature gradient between layers exceeds a critical lapse rate. In such cases of convective instability, a 6.5°C km^{-1} lapse rate is assumed. This lapse rate matches that commonly observed in the atmosphere. With the assumptions of a constant relative humidity and energy conservation the model iterates to a stable equilibrium radiative-convective temperature profile. Sarachik (1978) explicitly included a hydrologic cycle in a 1D-RD model and his results support the assumption of a constant relative humidity. The vertical distribution of relative humidity was taken from Manabe and Wetherald.

The specific humidity distribution assumed by Manabe and Wetherald requires some discussion. For a *clear* atmosphere at 35°N and relative to an equilibrium equinoctial temperature distribution calculated using their radiative-convective scheme, the relative humidity distribution was consistent with a precipitable water distribution of 1.78 cm. However, if clouds completely occupied the tropospheric slabs 913–854, 632–549 and 381–301 mb, the precipitable water content rises to 2.62, 2.01 and 1.80 cm, respectively.[4] These estimates may be compared with the observed mean values of 1.7, 1.8 and 2.1 cm for the Southern Hemisphere stations of Laverton (37°S, 144°E), Nowra (35°S, 150°E) and Lord Howe Island (31°S, 159°E).[5] Given that the three stations reside within the low cloudiness subtropics, the theoretical and observed values compare quite well which lends some confidence to the Manabe-Wetherald assumption.

The pure radiative equilibrium profile for the latitude in question was assumed as the initial temperature condition. Equilibrium is assumed when the net flux at the top of the atmosphere approaches constancy.

The neglect of the evolving oceanic thermal state [itself a strong function of both radiative heating and dynamic stirring (Webster and Lau, 1977)] is likely to be significant in the middle and high latitudes where the solar heating and the ocean temperature are out of phase. Although ignored in the present study, the omission may be remedied in a crude fashion by the application of a fixed surface temperature pertaining to the particular time of year. Such a technique was used by Manabe and Möller (1961) in the calculation of hemispheric equilibrium temperature cross sections with some success.

The omission of large-scale dynamic transports imposes restrictions on the determination of a realistic temperature profile particularly in the winter hemisphere where dynamic heat fluxes are largest. In order to assess the importance of the dynamic effects, the equilibrium profile for January at 35°N was calculated with the 1D-RC without dynamic effects and with total dynamic heat transports obtained from the climatological data of Oort and Rasmussen (1971). The two equilibrium profiles are shown on Fig. 3. The heat added to the system by the climatological dynamic heat transports is subject to radiative and convective adjustment by the model.

[4] The calculations with the cloud slabs was made using the model discussed in this paper. Saturation was assumed in the cloud layers.

[5] Data obtained from *Precipitable Water Statistics, Australia: Monthly Statistics of Precipitable Water between the Surface and 400 mb at 2300 GMT*, 1958–1969, by C. L. Pierrehumbert, Commonwealth of Australia, Bureau of Meteorology, Meteorological Summary. Obtainable from the Director, Bureau of Meteorology, Melbourne.

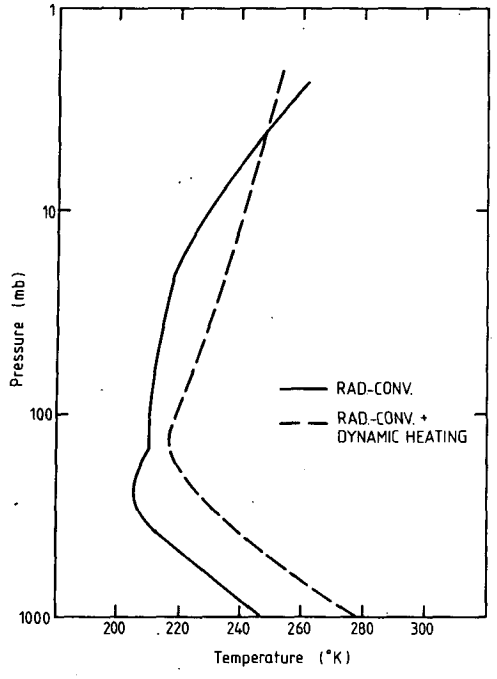

FIG. 3. Equilibrium temperature profile for 35°N in January calculated using the one-dimensional radiative convective model (solid curve). Modified profile which includes dynamic sensible heat convergence is shown as the dashed curve.

Equilibrium profiles for cases with and without the addition of the climatological heating are shown in Fig. 3. In the following sensitivity studies the appropriate climatological dynamic heating determined from Oort and Rasmussen will be included. However, it should be noted that the inverse feedback, the change of the dynamic effects relative to changes in the system structure for example by changes in cloud amount, cannot be included in so simple a model. Perhaps because of this truncated feedback, the sensitivity of the model structure appears independent of the dynamic heating. That is, dynamic heating added to the system in the manner described here provides only a first order correction to the system.

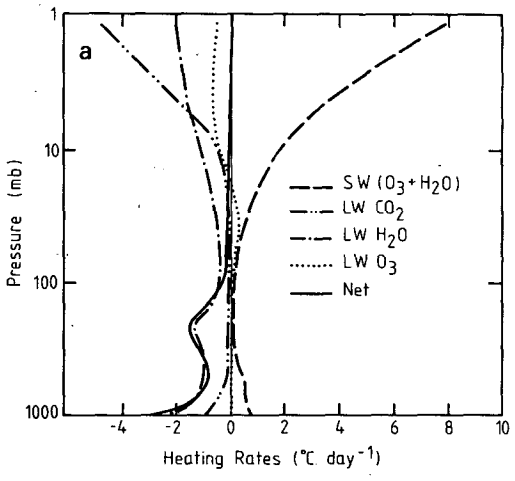

FIG. 4a. Vertical profiles of the various equilibrium diabatic heating rates (K day^{-1}) for the clear sky case (with climatological dynamics) shown in Fig. 3.

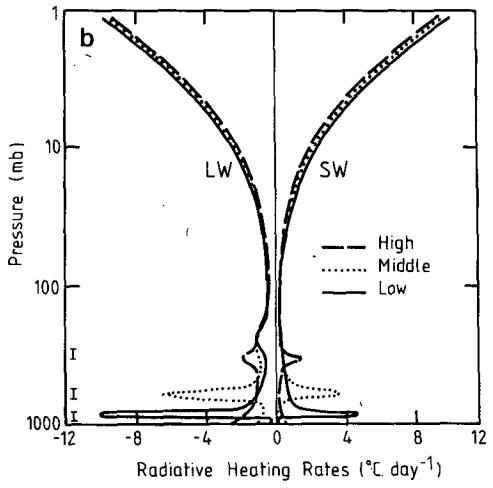

FIG. 4b. Vertical profiles of the total longwave, the total shortwave and the net diabatic heating rates (K day^{-1}) for overcast high, middle and low cloud. Liquid water paths for the three cloud species are 140, 140 and 20 g m^{-2}, respectively. Vertical bars denote the extent of the cloud decks.

6. Results

a. Heating rate profiles

The thermal structure of an atmospheric column is determined by the interplay of a number of diabatic heating functions and a response to that heating. In the simple structures discussed here, the response is accomplished by convective adjustment.

The vertical profiles of the equilibrium diabatic radiative heating rates for a clear atmosphere at 35°N in winter are shown in Fig. 4a and are quite similar to those obtained by Manabe and Strickler (1964). In the stratosphere and lower troposphere considerable heating occurs due to O_3 and H_2O shortwave absorption, respectively. Strong emission occurs in the stratosphere in the 15 μm CO_2–H_2O overlap region and this provides the largest compensation to the O_3 shortwave heating. With the addition of weak cooling by the 9.6 μm O_3 band and H_2O, the stratosphere appears in radiative equilibrium. In the troposphere, the total heating curve is principally determined by the H_2O cooling. The greatest difference from the Manabe-Strickler profiles occur in the lower troposphere where the inclusion of the *e*-type absorption in the atmospheric window region in the present study has resulted in enhanced cooling.

Fig. 4b shows the total longwave and shortwave

heating profiles as a function of pressure for three cloud types. Overcast conditions were stipulated. Low cloud (water path of 140 g m^{-2}) was assumed to occupy the 913–854 mb slab, middle cloud (140 g m^{-2}) the 632–549 mb slab, and high cloud (20 g m^{-2}) the 381–301 mb slab. A surface albedo of 0.102 was assumed. Each cloud species exhibits considerable longwave cooling and shortwave heating averaged in depth through the cloud so that the total heating of the cloud is a composite of two compensating quantities of similar magnitude. The decrease in longwave cooling of the cloud with increasing cloud height is a direct result of the clouds lower emitting temperature. Low-level clouds tend to cool most strongly since the upward flux at the cloud top exceeds the net input at its base. As the cloud base rises, the net longwave input at the base increases, whereas at the cloud top the cooling decreases (Stephens, 1980; Webster and Stephens, 1980).

The corresponding temperature profiles are shown in Fig. 4c. In the upper stratosphere there is little difference between the three cloud cases. However, in the lower stratosphere heating is apparent in the cloudy atmospheres due to the enhanced absorption of shortwave radiation reflected from the cloud top. Above each cloud layer is a distinct inversion which was absent in the results of Manabe and Wetherald and Manabe and Strickler. The strength of the inversion appears to match the longwave cooling noted in Fig. 4b. The development of stable layers in the vicinity of cloud decks has observational justification (Stephens *et al.*, 1978) although the magnitude of the model inversions may be excessive; a problem associated with the ignoring of fully interactive large-scale dynamics and cloud physics. One might expect either process to rapidly remove such inversions.

The existence of the cloud decks appears to have

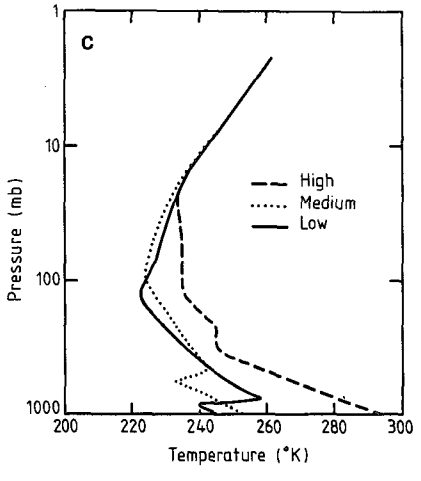

FIG. 4c. Vertical profiles of the equilibrium temperature (K) of the three cloud cases shown in Fig. 4b.

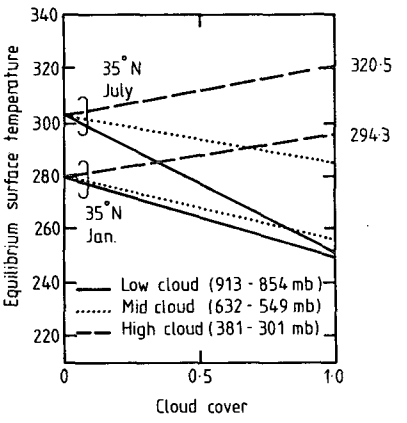

FIG. 5. Equilibrium surface temperature distribution (K) as a function of cloud amount for the low, middle and high cloud cases using winter and summer solstice conditions at 35°N. Liquid water paths for the three cloud species are 140, 140 and 20 g m^{-2}, respectively.

the effect of altering the mean temperature of the troposphere. Using the surface temperature as a guide (see the dashed curve of Fig. 3), the high cloud layer has tended to cause a 12 K warming compared to the clear case, whereas low and middle clouds have cooled the surface by over 25 K.

b. Surface temperature–cloud character relationships

Fig. 5 shows the equilibrium temperature of the earth's surface as a function of cloud amount for January and July at latitude 35°N although the nonlinear effects of the finite geometry of partial cloud cover have been ignored. Early 1D-RD models which included specified cloud layers (e.g., Manabe and Wetherald, 1967) found that most clouds caused a decrease of the surface temperature because the loss of energy by cloud-top reflection is greater than the enhanced increase of energy at the surface by thermal emission from the cloud. Fig. 5 supports the result for the optically thick low- and middle-level clouds. However, the optically thin high cloud (w = 20 g m^{-2}) produces a substantial surface temperature increase for both the January and July cases relative to the corresponding clear-sky surface temperature. This is consistent with the expectations of Manabe and Wetherald (1967) for thin cirrus where the loss of shortwave energy by cloud reflection does not balance or dominate the enhanced cloud longwave emission and with Cox (1971) who interpreted the Manabe and Wetherald results, with the aid of longwave radiative observations, to suggest that high-altitude, low-latitude cirrus may cause surface warming.

Fig. 6 shows the difference in surface temperature between clear and overcast skies for the three cloud species as a function of cloud-water or ice-water

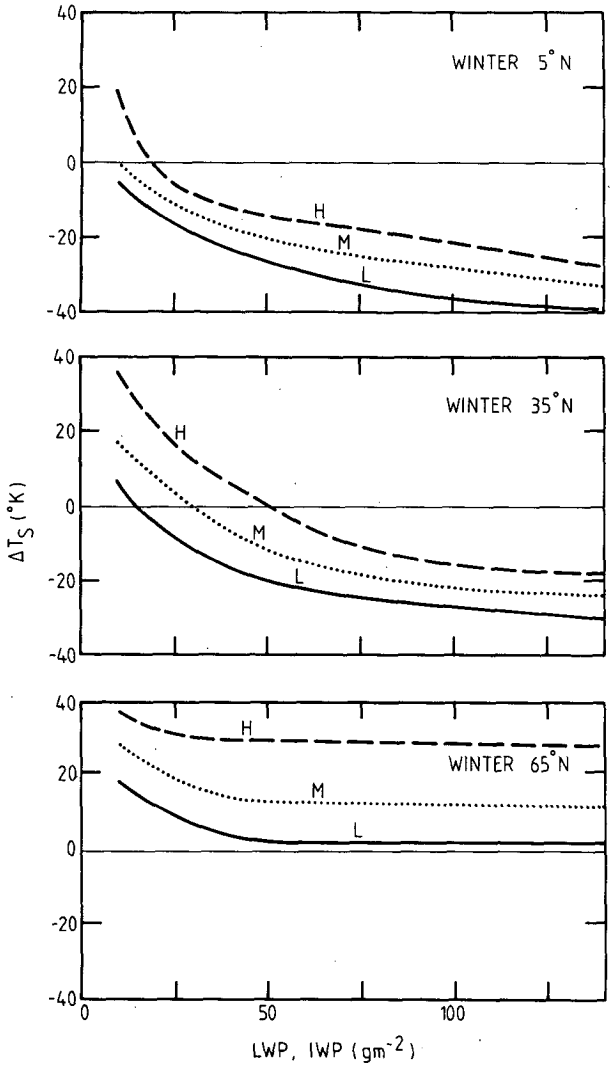

FIG. 6. Surface temperature difference (ΔT_s) between clear and overcast conditions as a function of water or ice-water path (g m^{-2}) for the three cloud layers defined in Fig. 5. Results for 5, 35 and 65°N in winter are shown with a surface albedo of 0.102.

path. Distributions for three latitudes are shown and winter insolation values are assumed. Generally, only high optically thin clouds tend to produce strong surface warmings at all latitudes, whereas at high latitudes all cloud species irrespective of water path tend to warm the surface relative to clear-sky conditions.

The curves of Fig. 6 suggest a strong role for cloud-water path in determining whether or not the cloud layer induces a surface warming or cooling. For a given surface albedo, the surface temperature in clear-sky conditions is determined by the degree of shortwave and longwave input at the surface. Surface warming will occur if the enhanced longwave input at the surface by the introduced cloud outweighs the loss of energy by shortwave cloud reflection. Alternatively, surface cooling occurs when cloud reflection dominates.

From Fig. 1a it is obvious that the numerical difference between cloud emittance and cloud albedo is greatest for thin clouds. For example, a cloud with a water path of 20 g m^{-2} possesses a cloud albedo of 0.36 and the effective emittance is 0.9 such that longwave enhancement at the surface dominates and the surface warms. Small increases in water path cause large increases in cloud albedo but only small changes in emissivity so that for only slightly thicker clouds shortwave reflection tends to dominate and the clouds become net coolers of the surface.

The latitudinal variation of the surface temperature change may be understood using similar arguments. At low and middle latitudes, the solar input at the surface in the clear-sky case tends to dominate the surface energy balance. Thus, except for clouds possessing a low albedo and a high emittance all clouds will cause surface cooling. However at high latitudes, the solar input is so small that the enhancement of the longwave flux at the surface by the introduced cloud dominates the surface balance. Consequently, all clouds irrespective of height in the winter polar regions tend to be net surface warmers.

At all latitudes the surface temperature effect is a strong function of cloud height. For a given water path the surface heating intensifies (or cooling reduces) with increasing cloud height. Such intensification arises because of the radiative energy loss to space. As the cloud top assumes the ambient temperature and as the cloud top represents the major radiating surface to space, the higher the cloud the smaller the energy loss. Consequently, as the subcloud temperature adjusts relative to the radiative loss to space, the subcloud and surface temperatures will be higher for (say) middle-level cloud than for low cloud if their water paths are identical.

In summary, equilibrium temperature structure appears to be extremely sensitive to both cloud character and the latitude of the cloud. As well as the height of the cloud being important, the optical properties of the cloud also determine the sense of temperature change at the surface. In essence it is the water path of the cloud which defines the particular albedo-emittance relationship and consequently the relative importance of the longwave and shortwave effects.

c. Temperature-surface albedo-cloud relationships

The variation of equilibrium surface temperatures as a function of surface albedo (a_s) for various cloud species and latitudes is shown in Fig. 7. For the clear case (heavy dashed curves) the relative importance of the longwave and shortwave inputs to the surface is easy to assess. The surface radiation balance may be written to first approximation as:

$$\sigma T_s^4 = S_0(1 - a_c)(1 - a_s) + \sigma\epsilon_A T_A^4 + \cdots, \quad (4)$$

where T_A is assumed to represent an effective radiating temperature of the atmosphere, a_c and a_s the cloud and surface albedos and S_0 the incoming solar flux at the top of the atmosphere. Thus for a steady T_A, the surface temperature will decrease rapidly with increasing a_s especially for clear-sky conditions (where $a_c = 0$ and ϵ_A is small) in low and middle latitudes (where S_0 is large). Generally, in cloudy skies (large a_c and ϵ_A) or at high latitudes (small S_0), we may expect variations in surface albedo to be of smaller importance.

However, the equilibrium temperature-surface albedo relationships in cloudy atmospheres are quite complex. From Fig. 7 it appears that at low and middle latitudes the surface temperature is nearly independent of surface albedo in the small albedo range but much more sensitive for higher albedos. The complicated form of the response leads to interceptions between the equilibrium temperature curves for the cloudy and clear cases. Thus, for a surface albedo less than some critical value (a_{sc}) a cloud of a given character will cool the surface relative to the clear atmosphere, whereas if $a_s > a_{sc}$ the tendency will be to warm the surface. All clouds in the winter high latitudes appear independent of surface albedo and therefore warm relative to the clear case. The latter independence is merely a manifestation of small insolation values at high latitudes and the dominance of the enhanced longwave effects due to the introduced cloud.

The critical surface albedo effect may be seen more clearly in Fig. 8 where equilibrium surface temperature differences between the clear and cloud cases are plotted. Generally, with increasing latitude (or zenith angle) the critical albedo for each species tends to decrease. For example, at 5°N the L(140) case possesses a critical albedo of 0.73, whereas at 35°N the critical value is reduced to 0.63. Over the same latitude range thick, a high-level cloud possesses values of 0.5 and 0.23. The critical albedos are summarized in Table 1 in order to emphasize the latitudinal dependence of a_{sc} illustrated above.

The following simple argument demonstrates the reason for the behavior noted in Figs. 7 and 8. If the criteria is used that the critical surface albedo is the albedo at which the surface temperatures for the clear and cloudy cases match, we can use (4) to obtain

$$a_{sc} = 1 - \frac{\sigma T_A^4(\epsilon_{A\theta} - \epsilon_{A\theta=0})}{S_0 a_c} + \cdots, \quad (5)$$

where $\epsilon_{A\theta}$ and $\epsilon_{A\theta=0}$ are the atmospheric emissivities of the cloudy and clear skies, respectively.

Noting the cloud albedo-emissivity relationships of Fig. 2 and assuming T_A is constant, it is obvious that for a given zenith angle (or alternatively a given

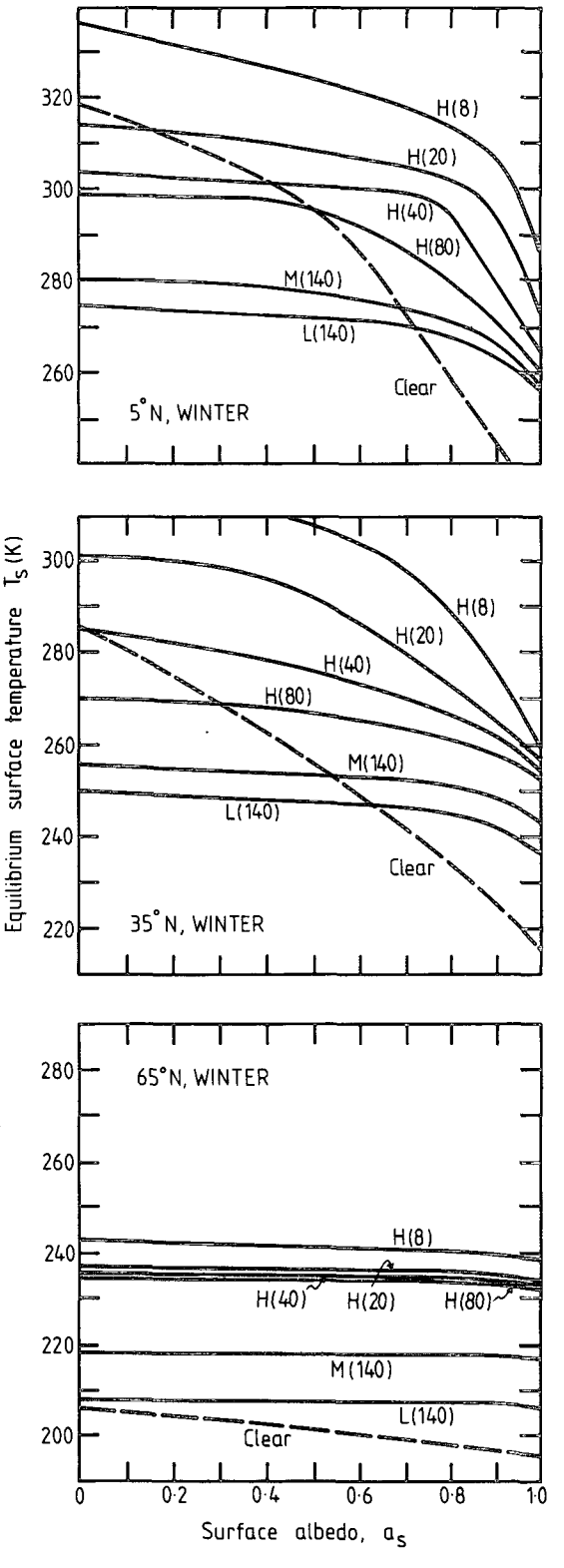

FIG. 7. Equilibrium surface temperature for various cloud case with given water path (solid lines) and the clear atmosphere (heavy dashed curve) as a function of surface albedo. Results for 5, 35 and 65°N in winter are shown. Clouds occupy the layers indicated in Fig. 5.

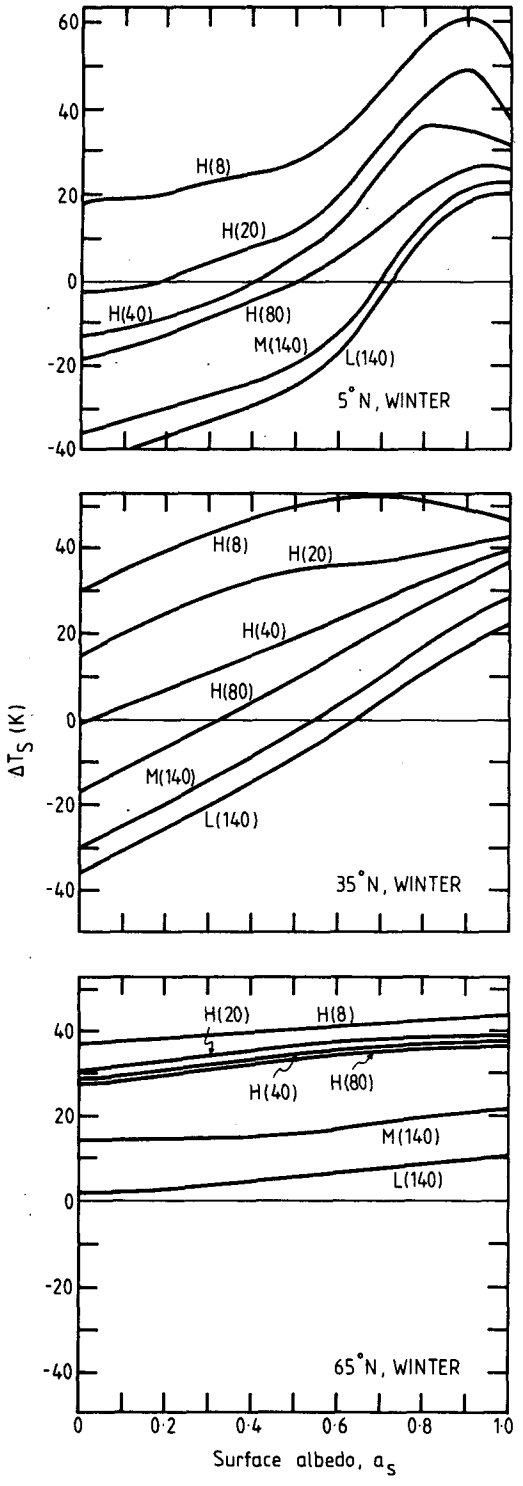

FIG. 8. Surface temperature difference (ΔT_s) between the clear and cloudy cases shown in Fig. 7. Results for 5, 35 and 65°N in winter are shown.

S_0) that the critical albedo for optically thick clouds (large a_c) will be larger than that for thinner clouds (small a_c). Similarly the critical surface albedo for a given cloud will increase with decreasing zenith angle (i.e., large S_0). The climatic significance of the effect will be discussed in the conclusions.

The vertical temperature structure is also a strong function of the surface albedo. This dependency is illustrated in Fig. 9 which shows the change in the equilibrium temperature profile between the $a_s = 0.102$ case and the $a_s = 0.3$, 0.5, 0.7 and 0.9 cases.

Three distinct domains of temperature change with increasing surface albedo are evident in the profiles. There are significant coolings at the surface and in the vicinity of the cloud layer and a warming in the upper levels, all of which increase in magnitude with increasing surface albedo. The surface cooling, already discussed, results from the energy loss at the surface by increasing shortwave reflection. The cooling in the cloud layer region in all three experiments results from the reduction of longwave radiation emanating from the cooler surface. This is most evident in the cloud layer as it is the region of maximum longwave absorption in the column. The warming in the upper layers results from the substantial increase in the upward flux of shortwave radiation and the subsequent increase of shortwave absorption.

7. Summary and conclusions

With the use of a simple one-dimensional radiative convective model, an attempt has been made to gage the effect of clouds on equilibrium thermal structures and sensitivities of simple climate systems. Because the one dimensionality of the model and the neglect of atmospheric and oceanic dynamics except for the effect of climatological eddy heat transports described in Section 5 the system response must be considered only a first approximation to real climate systems. However, as was found with an even simpler model (Stephens and Webster, 1979) sufficient sophistication has been included to be instructive in helping to emphasize the importance of certain physical mechanisms involved in the maintenance of climate states and in underlining certain problem areas which demand further study.

Table 2 summarizes the sensitivity of the surface temperature parametric variation as discussed in the preceding section. The sensitivity of T_s to changes in solar constant has been added for comparative purposes. Note that the solar constant sensitivity

TABLE 1. Critical albedos (a_{sc}) at which clouds transit from net surface coolers to net surface warmers.

	5°N	35°N	65°N
L(140)	0.73	0.64	—
M(140)	0.69	0.55	—
H(80)	0.50	0.23	—
H(40)	0.41	0.02	—
H(20)	0.19	—	—
H(8)	—	—	—

parameter is merely Schneider's (1972) "β climate factor". Using the table as a reference a number of points may be made.

(i) The surface temperature and vertical temperature structure is acutely sensitive to the cloud amount and cloud form (Figs. 4c and 5). Low clouds are seen to cool the surface, whereas high clouds tend to warm. Such behavior depends upon the longwave and shortwave optical properties of the cloud (the low clouds are radiatively black with large albedos and high clouds are grey and relatively poor reflectors) and the cloud height. The sensitivity of the model to changes in the amount of low and middle level clouds or thin high clouds is only a factor of 4 less than corresponding changes in solar constant. That is, a 4% change in cloudiness would produce the same change in surface temperature as a 1% change in solar constant.

(ii) The sensitivity of surface temperature to changes in the optical properties of clouds is large for optically thin clouds but less so for thick clouds (Fig. 6). Clouds with water paths ≥ 80 g m^{-2} possess relatively set optical properties (i.e., emissivity and albedo) for both short and longwave radiation, whereas for smaller water paths the optical properties vary rapidly. Sensitivity tends to decrease with decreasing insolation due to the diminishing influence of shortwave effects and the dominance of the enhanced longwave absorption at the surface from the cloud layer.

(iii) The temperature structure of an atmospheric column is acutely dependent on the magnitude of the surface albedo (Figs. 7, 8 and 9). Temperature sensitivity to changes in surface albedo decreases with latitude because of the decreasing importance of the shortwave radiation. Depending on the cloud character, there may be one surface albedo (a_{sc}) at which the surface temperature for the clear and cloudy cases is identical. For surface albedoes smaller than a_{sc} the cloud will cool the surface, whereas for larger albedos the cloud will warm the surface. The sensitivity of temperature to surface albedo is similar to that for the solar constant variations (see Table 2).

Generally, the results related to the role of cloud amount and cloud type [(i) and (ii) above] corroborates the findings of Manabe and Wetherald (1967). The major differences lies in the cloud optical property parameterization used. Manabe and Wetherald, who use a constant cloud albedo, state that it is the degree of blackness which determines whether a cloud will warm or cool the surface. Our study allows water path of a cloud at a given height to be established as the dominating parameter to which we relate both albedo and emissivity.

In an earlier study, Stephens and Webster (1979) hinted at the care that is necessary in the formulation of models in which radiative processes and cloud-radiative feedbacks were important. This includes models dealing with processes involving climate time-scales or even models dealing with

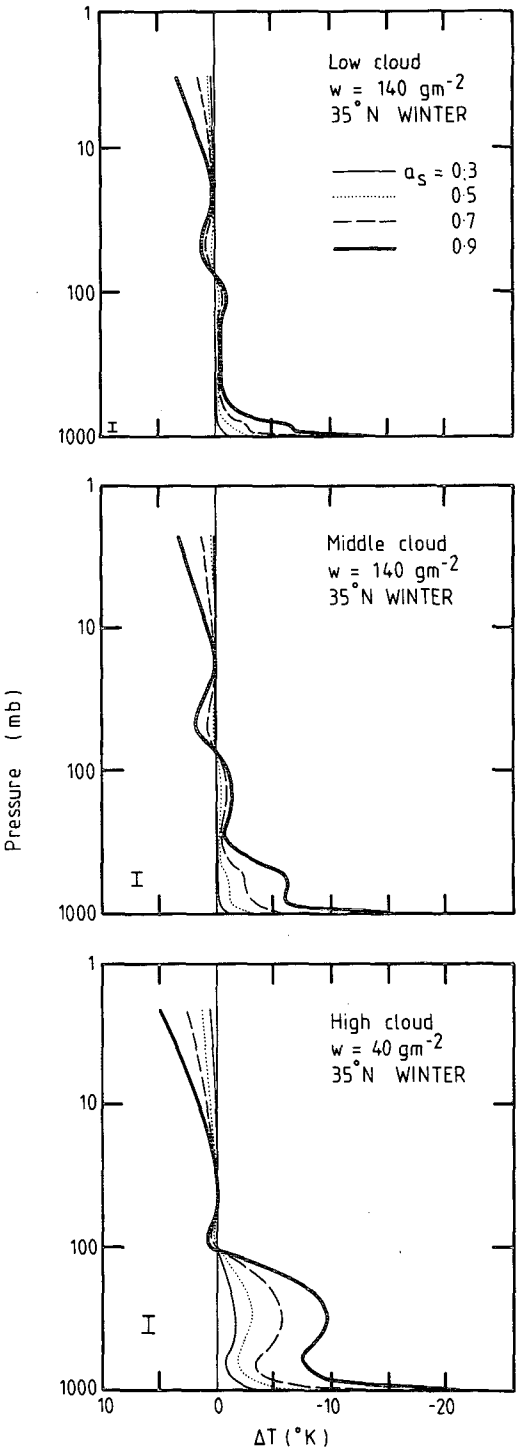

FIG. 9. Variation of the vertical temperature structure with surface albedo for low, middle and high cloud decks at 35°N in winter. The curves show the temperature difference (K) between equilibrium profiles calculated using surface albedos of 0.102 and those indicated.

TABLE 2. Surface temperature sensitivities to changes in various parameters at 35°N.

	Sensitivity $\frac{\alpha}{100}\frac{dT_s^*}{d\alpha}$				
Parameter α	Clear	L(140)	M(140)	H(40)	H(8)
Solar constant	+1.26	+1.20	+1.20	+1.25	+1.27
Cloud amount	—	−0.28	−0.22	+0.04	+0.26
Surface albedo					
$a_s < 0.5$	−0.8	−0.13	−0.17	−0.30	−0.46
$a_s > 0.7$	−0.9	−0.14	−0.18	−0.40	−1.20

* Sensitivity to ozone variation is calculated in the following manner:

$$\frac{\alpha}{100}\frac{dT_s}{\alpha\alpha} \approx \frac{\Delta T_s}{100[(\alpha_2 - \alpha_1)/\bar{\alpha}]},$$

where α_1, α_2 and $\bar{\alpha}$ are the McClatchey *et al.* (1972) total ozone concentration values which are 0.45, 0.227 and 0.36 cm NTP, respectively.

tropical phenomena of considerably smaller time scales (Webster and Stephens, 1980). By relaxing the constraints of the Stephens-Webster model, the present study allows further and more specific conclusions to be drawn.

(i) The sensitivity of equilibrium temperature to the amount of cloud indicates the necessity for careful cloud parameterizations. The results of the present model substantiate the findings of Stephens and Webster (1979). Not only must the amount of cloud be carefully gaged in a model scheme but also the cloud radiative properties and cloud heights. For example, Fig. 7 suggests distinct dependences on the height of cloud and on cloud-water path, especially for optically thin clouds. For optically thicker clouds, the optical properties are less variable but the establishment of the cloud height remains critical.

(ii) The acute sensitivity of the model structure to surface albedo variations and cloud optical property indicates the need for careful parameterization of both effects. Over continental regions and in ocean areas in winter large variations in the surface albedo may occur in both space and time (see Webster and Chou, 1980) such that the critical albedos calculated in Section 6*c* fall within realisable limits.

(iii) As the surface albedo is increased, clouds tend to either become net warmers of the surface or reduce their degree of cooling. Consequently, if cloud amount is either independent of temperature change or increases with the cooling of the troposphere or the surface, cloud will tend to act as a climate buffer. That is, the surface albedo-cloud effect will tend to be negative. On the other hand, if cloud amount decreases with decreasing temperature the surface albedo-cloud effect will tend to be positive and any decrease in surface temperature caused by an increase in surface albedo would be emphasized. Consequently, the relationship of temperature change to cloud amount would appear central to the surface temperature-albedo schemes which depend primarily on surface temperature (Faegre, 1972; Webster and Chou, 1980).

The phenomenological interpretations of the results of the study listed in (iii) underline the necessity for the determination of whether or not cloud is related to or is independent of the temperature structure of the atmosphere or surface conditions. Such an interpretation is substantiated by Paltridge (1980). It is unlikely that such a relationship will be simple to develop as cloud amount and character will depend strongly on dynamical state and synoptic situation on which the temperature structure also is partially dependent. However, without such a relationship models of the degree of sophistication developed here can be used at best to hint at the sensitivities of a real system and not as forecast models of climate change.

Within the limitations of the model noted above, a number of worthwhile studies can be recommended. The present study relates to temperature sensitivities relative to a surface with small thermal inertia and as such is not appropriate to ocean surfaces. In order to overcome this limitation, the advective mixed-layer model of Webster and Lau (1977) is being attached to a model similar to that described here. Also, the results described above pertain to clear- or overcast-sky conditions. The extension of the study to consider partial sky cover in a manner which encompasses the nonlinear effect due to finite geometrics will allow the testing of the climate feedback hypotheses described above.

Acknowledgments. Part of this work was carried out while one of us (GLS) was on leave from CSIRO at the Department of Atmospheric Sciences, Colorado State University. Partial support by NSF Grant ATM-7807148 is appreciated.

REFERENCES

Budyko, M. I., 1969: The effect of solar radiation variations on the climate of the earth. *Tellus*, **21**, 61–69.

Cess, R. D., 1976: Climate change: An appraisal of atmospheric feedback mechanisms employing zonal climatology. *J. Atmos. Sci.*, **33**, 1831–1843.

Cox, S. K., 1971: Cirrus clouds and the climate. *J. Atmos. Sci.*, **28**, 1513–1515.

——, and K. T. Griffith, 1979: Estimates of radiative divergence during Phase III of GATE. Part I: Methodology. *J. Atmos. Sci.*, **36**, 566–575.

Faegre, A., 1972: An intransitive model of the earth-atmosphere-ocean system. *J. Appl. Meteor.*, **11**, 4–6.

Goody, R. M., 1964: The transmission of radiation through an inhomogeneous atmosphere. *J. Atmos. Sci.*, **21**, 575–581.

Hartman, D. L., and D. A. Short, 1980: On the use of earth radiation budget statistics for studies of clouds and climate. *J. Atmos. Sci.*, **37**, 1233–1250.

Hunt, B. G., 1978: On the general circulation of the atmosphere without clouds. *Quart. J. Roy. Meteor. Soc.*, **104**, 91–102.

Hunt, G. E., V. Ramanathan and R. M. Chervin, 1980: On the role of clouds in the general circulation of the atmosphere. *Quart. J. Roy. Meteor. Soc.*, **106,** 213–215.

Kuriyan, J. G., Z. Shippony and S. K. Mitra, 1977: Transmission function for infrared radiative transfer in an inhomogeneous atmosphere. *Quart. J. Roy. Meteor. Soc.*, **103,** 511–517.

Lacis, A., and J. E. Hansen, 1974: A parameterization for the absorption of solar radiation in the earth's atmosphere. *J. Atmos. Sci.*, **31,** 118–133.

Manabe, S., and F. Möller, 1961: On the radiative equilibrium and heat balance of the atmosphere. *Mon. Wea. Rev.*, **89,** 503–532.

——, and R. F. Strickler, 1964: Thermal equilibrium of the atmosphere with convective adjustment. *J. Atmos. Sci.*, **21,** 361–385.

——, and R. J. Wetherald, 1967: Thermal equilibrium of the atmosphere with a given distribution of relative humidity. *J. Atmos. Sci.*, **24,** 241–259.

Malkmus, W., 1967: Random Lorentz band model with exponential-tailed S^{-1} line intensity distribution function. *J. Opt. Soc. Amer.*, **57,** 323–329.

Ohring, G., and P. F. Clapp, 1980: The effect of change in cloud amount on the net radiation at the top of the atmosphere. *J. Atmos. Sci.*, **37,** 447–454.

Oort, A. J., and E. Rasmussen, 1971: *Atmospheric Circulation Statistics*. NOAA Prof. Pap. No. 4, U.S. Dept. of Commerce, 323 pp.

Paltridge, G. W., 1980: Cloud-radiation feedback to climate. *Quart. J. Roy. Meteor. Soc.* (in press).

——, and C. M. R. Platt, 1976: *Radiative Processes in Meteorology and Climatology*. Elsevier, 318 pp.

Platt, C. M. R., D. W. Reynolds and N. L. Abshire, 1980: Satellite and lidar observations of the albedo, emittance and optical depth of cirrus compared to model calculations. *Mon. Wea. Rev.*, **108,** 195–204.

Rodgers, C. D., 1967: The use of emissivity in atmospheric radiation calculations. *Quart. J. Roy. Meteor. Soc.*, **93,** 43–54.

——, and Walshaw, C. D., 1966: The computation of infrared cooling rate in planetary atmospheres. *Quart. J. Roy. Meteor. Soc.*, **92,** 67–92.

Sarachik, E. S., 1978: Tropical sea surface temperature: An interactive one-dimensional atmosphere-ocean model. *Dyn. Atmos. Oceans*, **2,** 455–469.

Schneider, S., 1972: Cloudiness as a global feedback mechanism: The effects on the radiation balance and surface temperature on variations in cloudiness. *J. Atmos. Sci.*, **29,** 1413–1422.

Stephens, G. L., 1978: Radiative properties of extended water clouds. II: Parameterizations. *J. Atmos. Sci.*, **35,** 2123–2132.

——, 1980: Radiative properties of cirrus cloud in the infrared region. *J. Atmos. Sci.*, **37,** 435–446.

——, and P. J. Webster, 1979: Sensitivity of radiative forcing to variable cloud and moisture. *J. Atmos. Sci.*, **36,** 1542–1556.

——, and K. J. Wilson, 1979: The response of a deep cumulus convective model to changes in radiative heating. *J. Atmos. Sci.*, **37,** 421–434.

——, G. W. Paltridge and C. M. R. Platt, 1978: Radiative properties of extended water clouds III. Observations. *J. Atmos. Sci.*, **35,** 2133–2143.

Webster, P. J., and K. M. W. Lau, 1977: A simple ocean-atmosphere climate model: Basic model and a simple experiment. *J. Atmos. Sci.*, **34,** 1063–1084.

——, and L. C. Chou, 1980: Seasonal structure of a simple monsoon system. *J. Atmos. Sci.*, **37,** 354–367.

——, and G. L. Stephens, 1980: Tropical upper-tropospheric extended clouds: Inferences from Winter MONEX. *J. Atmos. Sci.*, **37,** 1521–1541.